EFDA–JET–CP(12)06/27

I. Nunes, V. Riccardo, P.J. Lomas, P. de Vries, D. Alves, G. Arnoux, S. Devaux, T. Farley, M. Firdaouss, S. Jachmich, G. Matthews, C. Reux, K-D Zastrow and JET EFDA contributors

Be Tile Power Handling and Main Wall Protection

Be Tile Power Handling and Main Wall Protection

I. Nunes[1], V. Riccardo[2], P.J. Lomas[2], P. de Vries[3], D. Alves[1], G. Arnoux[4], S. Devaux[2], T. Farley[5], M. Firdaouss[6], S. Jachmich[7], G. Matthews[2], C. Reux[8], K-D Zastrow and JET EFDA contributors*

JET-EFDA, Culham Science Centre, OX14 3DB, Abingdon, UK

[1]Associação EURATOM/IST, Instituto de Plasmas e Fusão Nuclear, Instituto Superior Técnico, Universidade Técnica de Lisboa, 1049-001 Lisboa, Portugal
[2]EURATOM-CCFE Fusion Association, Culham Science Centre, OX14 3DB, Abingdon, OXON, UK
[3]FOM Institute Rijnhuizen, Association EURATOM-FOM, Nieuwegein, the Netherlands
[4]Max-Planck-Institut für Plasmaphysik, EURATOM-Assoziation, 85748 Garching, Germany
[5]Bristol University, Tyndall Avenue, Bristol, BS8 1TL, UK
[6]CEA, IRFM, F-13108 Saint-Paul-lez-Durance, France
[7]Laboratoire de Physique des Plasmas-Laboratorium voor Plasmafysica, Association EURATOMBelgian State, ERM/KMS, B-1000 Brussels, Belgium
[8]Ecole Polytechnique, CNRS, 91128 Palaiseau Cedex, France
** See annex of F. Romanelli et al, "Overview of JET Results", (24th IAEA Fusion Energy Conference, San Diego, USA (2012)).*

Preprint of Paper to be submitted for publication in Proceedings of the 24th IAEA Fusion Energy Conference (FEC2012), San Diego, USA 8th October 2012 - 13th October 2012

ABSTRACT

In the 2010 shutdown, JET has changed its main chamber limiters and divertor from Carbon Fiber Composite to beryllium and tungsten respectively, to mimic the ITER main chamber and divertor and study the impact of this change in the plasma behaviour as well as to study the power handling of these materials for high power operation. This change required a complete redesign of the limiter tiles and of the protection system to avoid melting since the melting temperature for Be is 1249^{o}C in contrast to the 3500^{o}C sublimation temperature of the CFC. The shaping of the tiles surface for optimisation of the power handling, avoidance of exposed edges over 40μm wetted height and the use of rigorous methods to ensure true implementation allowed us to achieve very good power handling and the expected design values has been achieved. The corroboration of the design was done with a field line following code and experimentally by using limiter plasmas with additional heating (maximum of ~5MW for 7s) with the contact point in both the inner and outer limiter and X-point plasmas with additional power of ~25MW for 3s. The results show good agreement with the calculations and the main chamber power handling has achieved and possibly exceeded the design targets. The wall and divertor protections have also been improved with a vessel temperature map system that collects temperature measurements from near infra-red cameras and computes in real time the temperature in the various wall components. Overall, the "JET ITER-like Wall project" has been very successful.

1. INTRODUCTION

The JET ITER-like Wall (ILW) is the first tokamak experiment to combine beryllium (Be) for the main chamber limiters and tungsten (W) for the divertor, materials foreseen for the active operational phase in ITER because of its expected low tritium retention relative to the carbon fiber composite (CFC) material [1,2]. Whilst at ITER the main chamber is completely cover by panels made of bulk Be and the divertor made of bulk W, at JET only the poloidal limiters are made of bulk Be. However, the first wall at ITER is shaped, which makes the assessment of the Be tiles power handling at JET an important contribution to the design of the ITER first wall. The cladding tiles, recessed from the main limiters, are made of W-coated CFC for the shine-through areas or Be-coated inconel for recessed areas, not exposed to plasma. The divertor, composed by 7 tiles, 4 vertical and 3 horizontal is made of W coated CFC except tile 5 where the outer strike lies for most of the operational scenarios, which is made of bulk W. The power handling of the bulk W divertor is presented separately [3] and only the main chamber Be poloidal limiters will de discussed in this paper.

Be components were previously used at JET in the period between 1990-1995, including the toroidal belt limiters [4,5,6,7]. Here, the tiles were simply castellated with exposed edges, not optimised for power handling. Because the limiters are required to have good power handling for start-up limiter operation as well as handling high power densities due to high power input (P_{in} > 34 MW) in diverted ELMy H modes for times of ~10s, it was decided to shadow the edges within a tile and from tile to tile. The design of the new bulk Be tiles for the different limiters (3 poloidal

limiters) was constrained by several technical objectives, the reuse of the existing supports for the tiles, originally designed for the CFC tiles, and compatibility with fully remote handling installation.

The tiles are segmented to reduce the eddy current forces and castellated to avoid thermal stress cracking (e.g. tile for the outer poloidal limiter in figure 1) [8,9]. Within a tile, only the poloidal edges of the castellations of the outer segments are shadowed by tile shaping, the edges in the central segment are not shadowed. A limit of 40μm for the exposed toroidal edge, determined from sensitivity studies, and a minimum achievable gap between castellations of 350μm determine the maximum slope for the central block where the edges are not shadowed. The shadowing of the exposed edges from tile to tile for the low field side (LFS) limiters (wide poloidal limiter – WPL) is done by chamfering the tile surface in the poloidal direction as shown in figure 1. The exposed edges from tile to tile at the high field side (HFS) limiters (inner wall guard limiter – IWGL) are not shadowed, since the expected power density at the surface is higher than the one expected at the exposed edges in the toroidal facing surface. The tile surface is designed using polynomial equations and the power density profile is calculated analytically [10]. These calculations do not take into account the toroidal curvature of the flux surfaces for the LFS, or the shadowing effect from the adjacent limiters for both LFS and HFS for determining the maximum power and its toroidal position. The scrape-off length values of 10mm (LFS) and 20mm (HFS) for ohmic and L-mode limiter plasmas were used and an exponential decay of power density with radius and scrape-off length is assumed. Empirically determined values of the scrape-off layer length were found to be in the range λ_q = 0.4-0.8 cm [4] and more recently, dedicated experiments were performed to determine the scrape-off layer length by using infra-red camera and Langmuir probe measurements. For the LFS the average value was found to be 8mm whilst at the HFS, λ_q varies from 20 to 80mm for small and large field line angle respectively [11].

Because of technical constraints, the power density profile for the IWGL and WPL are not similar. While for the outer limiter it is possible to achieve a constant power density profile along the tile surface, the inner limiter has a maximum power density towards the wings of the tile, degrading the limiter power handling. The limiters are designed for a single field-line helicity at the LFS and double helicity at the HFS. A numerical field line following code (CFPFLU)[12] was used to verify the analytical solutions with very good qualitatively and quantitatively agreement. To corroborate the design of the tiles, experiments were performed with temperatures close to the design limits. These include H-mode diverted plasmas with varying distance to the limiters and limiter plasmas with additional heating and varying field line. The low melting point of the beryllium in the main chamber plasma facing components, the risk of delamination of the tungsten coating and the temperature threshold at which the bulk tungsten re-crystallises (1200^{o}C) of the divertor tiles, requires the surface temperature of these components to be monitored in real time to avoid overheating and eventually melting. Together with the upgrade of the existing protection systems, a new system that computes in real time the surface temperature of the various components has been successfully used. In this paper we describe the design methodologies applied to JET's ITER-like

Wall (ILW), many of which have been adopted by ITER, and the experimental evaluation of their effectiveness. This experience has direct relevance
to the ITER plasma facing components (PFCs) showing that stringent criteria for exposure of edges at the castellation scale and penetration of field lines in extreme off-normal configurations has to be considered.

2. EXPERIMENTAL VALIDATION OF POWER HANDLING

2.1. PEAK POWER DENSITY

The plasma parameters that influence the maximum surface power density and the position of this maximum through their effect on field lines connection length hence shadowing from the adjacent limiters are λq, the angle of incidence in the PFCs of the magnetic field line (ζ) and elongation (κ). In order to look at the Be tiles power handling and its dependence with these parameters, limiter plasmas on both HFS and LFS were performed. Additional heating using neutral beam injection (NBI) is used to increase the power at the scrape-off layer therefore increasing the power density at the tiles surface. The magnetic field line angle (ζ) varied from 3.5 to 12.5 degrees at the HFS and from 6 to 18.2 degrees at the LFS, achieved by varying q_{95} and to vary elongation, two shapes with $\kappa \sim 1.25$ and ~ 1.5 were used (figure 2). In order to avoid X-point formation, it was not possible to increase the elongation further than 1.5. Measurements of the surface temperature and power density are taken from IR [11] measurements.

Figure 3 shows a comparison between the two methods, numerical [12] (PFCFLUX) (a) and analytical (c), used to design and check the power density of the Be tiles and the measured temperature (b). The magnetic equilibrium used experimentally in this example is taken from the PROTEUS code, which was used in the PFCFLUX code. As mentioned earlier, for the HFS, a power scrape-off length of 20mm is used for both calculations. The analytical solution includes the contribution from shadowing of the neighbouring limiters and the toroidal curvature of the field lines.

The patterns are reassuringly similar, a maximum peak heat-flux is observed towards the wings of the tile with a dip between the maximum and the second lower maximum at the apex of the tile.

Experimental values of power density can be obtained from the IR measurements by solving the 1D nonlinear heat diffusion equations associated with the changing of the limiter surface temperature to calculate the deposited heat flux incident on each point of the surface of the limiter [11]. Figure 4 shows: (a) the power density calculated from the IR temperature measurements, (b) the toroidal profiles for the e-drift side, (c) the poloidal profiles at the centre (blue) of the limiter and the i-drift (black) and e-drift (red) side and (d) the analytically calculated toroidal profiles the power density with λ_q at the far SOL (blue), and near SOL (red) for an ohmic pulse with contact point in the IWGL with $\kappa = 1.31$, $P_{SOL} = 1.5$MW and $\zeta = 9.2^o$. The values of scrape-off length are taken from measurements [13]. The poloidal profiles (figure 4b) taken for the limiter tiles at the positions annotated in (a) (vertical lines) show an approximately constant maximum peak power along the length of the limiter, which is in line with the predicted values where the poloidal curvature of the

limiter is neglected. However, the predicted position of the maximum (from both analytical and numerical calculations) is further out, towards the tile wings as shown in figure 4d (red curve). Both profiles on the i- and e-drift side show a steep gradient of power density outside the apex, which can be explained by the effect of shadowing from the short connection length field lines of the adjacent limiters. The expected peak power density away from the contact point is closer to the apex than predicted (red curve). The predicted toroidal profiles on the e-drift side are determined using the measured average $\lambda_q = 43.9$mm and short distance between the adjacent limiters to determine the shadowing. In the e-drift direction because of the short distance between adjacent poloidal limiters the shadowing is dominated by the field lines with short connection length. The red curve in figure 4d shows that by including both λ_q, the predicted peak power density is ~1.5MW/m^2 at the apex and towards the tile wings. From the measurements, the poloidal power density profiles show a peak power density of 0.5MW/m^2 at the apex and at the tiles wings. However, the calculations in both cases do not fit the observations and the analytical and numerical calculations always show an overestimate of the power density. The power balance between IR measurements and power calculations ($P_{SOL} = P_{IN} - P_{rad}$-dW/dt) show a measured value a factor of 2 lower than the calculated P_{SOL} [11]. This would bring the discrepancy between predicted and measured power density to a maximum of ~1.5. Deposited layers on the limiters could also be an explanation, but no layer effect is observed in the IR temperature measurements. A simple explanation for the missing power may be that the radiation, due to recycling effects in the near SOL is higher than the measured one, which would overestimate P_{SOL}. Temperature calculations using the solution of the temperature distribution equation for a constant heat flux in a semi-infinite solid show good agreement with the measured temperatures at the outer limiters. To achieve the measured surface temperatures the fraction of radiated power fraction would have to be larger than the measured 20% for ohmic and NBI heated plasmas. Measurements at the i-drift side are more complicated to determine from the IR measurements and at the moment this data is not yet available. However, it is possible to see from the predicted profiles that there is an asymmetry on the position of the peak power at the wings. This movement of the peak further out on the i-drift side relative to the e-drift side is expected because of the geometry of the limiters, and the fact that the power load is not unevenly distributed on the limiters. In the i-drift side case, the contribution to the shadowing is due to the long connection length because the adjacent limiter is recessed which makes the tile wings more exposed. Because of the non-uniform distribution of the power density along the tile increases towards the wings, which is observed here.

1.1. EFFECT OF ELONGATION AND FIELD LINE ANGLE

Due to the non-uniform power density profile on the tile surface for the HFS limiters, shadowing becomes very important when designing the tile surface. For the LFS limiters, although not negligible, is less crucial. The effect of elongation and field line angle changes the shadow cast on a limiter from the adjacent limiters. The example of figure 5 shows the measured surface temperature and

temperature profiles for two pulses with $\zeta = 3.55^{o}$ and 8.06^{o} with elongation approximately constant. The effect of the field line angle on the shadowing is clearly observed. For Pulse No: 81872 where $\zeta = 3.55^{o}$, most of the limiter is shadowed by the adjacent limiters. As the field line angle increases (Pulse No: 81873 has a field line angle of 8.06^{o}) deeper penetration behind the tiles becomes possible exposing a larger region around the contact point and the peak power density is again found on the wings of the tile away from the contact point where the power handling degrades. The impact of elongation on the peak power density for the IWGL is similar to that of the field line angle. For small elongation, the peak power density is found near the apex of the tile, as the limiter ends determine the shadowing. As elongation increases, the peak power density increases and moves towards the wings of the tiles as the limiter ends get closer the last close flux surface. Figure 5 also shows an asymmetry on shadow cast on the limiter by the adjacent limiter between the i-drift side and the e-drift side. This is particular to JET and is due to the fact that the adjacent limiter (on the right hand side) that shadows this region is recessed and the field lines with short connection length cast no shadow on the limiter. By increasing elongation, the plasma curvature approaches that of the limiter and the ends of the limiter are exposed. Due to the tiles design, it is expected a decrease of the peak power density increasing elongation. Figure 6 shows the time traces for two plasmas with similar $\zeta = 9.7^{o}$ and P_{LOSS} with elongation of 1.26 and 1.5. The temperature rise for Pulse No: 82359 ($\kappa = 1.5$) is smaller than for Pulse No: 81754 ($\kappa = 1.26$). Extrapolating from the numerical simulations, it is expected a temperature rise of ~200^{o}C for low elongated plasmas and ~142^{o}C for high elongated plasmas. Measured temperatures are a factor of 4-7 lower than predicted as for the IWGL. This discrepancy is being investigated.

The assessment of the tiles design and validation of the assumptions has been tested by using plasmas with additional heating reaching surface temperatures of 920^{o}C as shown in figure 8. Operation of X-point diverted plasmas with P_{LOSS} of ~23MW for 3s and a gap of 5.6cm have also shown small increase of the surface temperature on both the inner and outer limiters confirming the good power handling of the limiters in diverted operation.

2. ILW ACTIVE PROTECTION

The limits on the surface temperature of the new Be tiles constrains limiter operation, sets the minimum gaps for diverted operation and requires active protection to guard against melting which, could seriously degrade the power handling and lifetime of the PFCs in JET and ITER. Three systems monitor the wall loads in real time; the wall load limiter system (WALLS) [15], the upgraded plant enable window system (PEWS2) and the new system, the vessel temperature map (VTM). WALLS, determines the topology and location of the plasma boundary based on real-time magnetic measurements. It controls the plasma clearance from the wall at various locations, including the positions of the magnetic strike points in the divertor region. It also models the power deposition and the thermal diffusion on individual plasma facing components using the information of the plasma current and the instantaneous injected power, thus monitoring the surface and bulk temperatures of

the PFCs. PEWS2 predicts the surface temperature and is responsible for insuring safe operation of the neutral beam heating system, i.e. checking the plasma has a minimum density and guaranteeing that the maximum injected energy allowed is not exceeded. If the surface temperature in any of the shine-through regions, PEWS2 can stop the respective PINIs and switch on others in order to keep constant the input power for the experiment or switch off the entire NBI system.

Finally, the VTM system was specifically designed to receive the data from the IR and near- IR cameras installed for the protection of the ILW. The monitoring of the surface temperature done with near infra-red cameras covers ~70% of the outer limiters, ~50% of the inner limiter, ~30% of tile 5 in the divertor and ~20% of the other tiles within a temperature range from 600^{o}C to 850^{o}C and from 850^{o}C to 1300^{o}C [13]. A defined set of regions of interest (ROIs) is analysed (figure 9a) and its measured temperature processed in real time by the VTM system. If any of the limits, defined by the operating instructions, are reached an alarm is sent to the Real Time Protection System (RTPS) [16] that coordinates the responses for the various systems issuing a request for an action that can be to stop the additional heating to reduce the heat loads on the PFCs or to safe terminate the plasma if the reduction of the additional heating was not successful (figure 9b).

These stops are programmable and designed to respond appropriately to the particular fault condition (hot spot location) for the specific scenario currently in use. These have been successfully used for the protection of the main chamber and are close to being fully commissioned. Additionally, there are also thermocouples in some of the tiles both in the poloidal limiters and divertor for post-pulse analysis and pyrometers looking at the lower hybrid and current drive antenna (LHCD), (not seen in figure 7) and the inner wall guard limiter in the region of the NBI shine-through (numbers 3 and 4 in figure 7).

The temperature range of the pyrometers is 350^{o}C–1300^{o}C. Coherence among systems is achieved by individual consistency checks and by the pulse schedule editor, the pre-pulse configuration tool [17]. Hot spots due to neutral beam re-ionisation power loads that are hard to predict with sufficient accuracy have been successfully detected and protective action taken. However, while deliberately exploring the limits of the limiter power handling (well above the originally predicted limits) damage to the tiles was observed (figure 8). Although the monitored temperature stayed below 800^{o}C, the temperature in the limiters not monitored must have reached far higher temperatures with one in view of a camera apparently releasing Be in bursts. Posterior inspection of the inner limiters have shown melting in two limiters. The melting has occurred close to the top of the limiter and has not affected normal operation with diverted plasmas or limiter plasma start-up. Possible causes are the toroidal misalignment of the limiters and/or the misalignment from tile to tile higher than the design specification. One other possible cause is the funnel effect thought to occur at the IWGL [11].

For the divertor, in addition to the cameras, pyrometers and thermocouple measurements are also available for protection. There was however an initial problem with false alarms due to hot dust particles moving around in the field of view. Effective algorithms have however now been developed which discriminates these from true bulk heating.

3. SUMMARY

The power handling of the HFS and LFS limiters is as expected and the impact on the overall performance of the Be limiters caused by misalignments, damage and other possible nonconformances appears to be minimal for normal operation. IR measurements show values for the measured power density at the tile surface a factor of 2-4 lower than the predicted values for the HFS and 4-7 for the LFS. Possible contributions for the discrepancy are the asymmetry observed in the power density measured between the i- and e-drift sides, toroidal asymmetry of the limiters and measurement errors and these are being investigated. The effect of field line angle and elongation on the shadowing is critical for the power handling of the HFS limiters.

For the outer limiter and because of the uniform power density profile along the tile, the peak power density does not depend strongly on the shadowing from the adjacent limiters, hence field line angle and elongation. However, a dependence of peak power density with elongation at the LFS is found which may indicate that the scrape-off length depends on the plasma poloidal curvature, which was not looked at during the dedicated experiments to determine experimentally the plasma scrape-off length.

The active protection put in place for operation of the ILW has been showed to prevent most of the pulses where the tiles surface temperature reaches the operational limits. Plasmas have also been successfully terminated in situations where it is hard to predict with sufficient accuracy the surface temperature of the tiles, such as hot spots due to neutral beam re-ionisation power loads. The programmable stop responses have been successfully used for the protection of the main chamber and are now fully commissioned.

The fact that although the active protection is fully operational for both the inner and outer limiters, it only covers 50% of the inner limiters and 70% of the outer limiters in the main chamber and possible misalignments larger than the design specifications have lead to melt damage during operation of limiter plasmas above the designed limits for the tiles power handling.

ACKNOWLEDGEMENTS

This work was supported by EURATOM and carried out within the framework of the European Fusion Development Agreement. The views and opinions expressed herein do not necessarily reflect those of the European Commission.

REFERENCES

[1]. Federici G. et al., Nuclear Fusion, **41**, 12R (2001) 1967;

[2]. Philipps V., Roth J., Loarte A., 30th EPS, St. Petersburg, July 2003, “Key Issues in Plasma-Wall Interactions for ITER: A European Approach”

[3]. Mertens, Ph et al., this conference

[4]. E. Deksnis, et al., Fusion Engineering and Design **37** (1997) 515

[5]. Loarte A, et al., Journal of Nuclear Materials **337-339** (2005) 816-820

[6]. E. Deksnis, et al., Journal of Nuclear Materials **176-177** (1990) 583
[7]. P.R. Thomas, et al., Journal of Nuclear Materials **176-177** (1990) 3
[8]. Riccardo V., et al., SOFT 2012
[9]. Thompson V. et al, Fusion Eng. Design Vol. **82**, issues 15-24, October 2007
[10]. Nunes I et al. Fusion Eng. Design Vol. **82**, issues 15-24, October 2007
[11] Arnoux, G. et al., this conference
[12]. Firdaouss M et al., EPS 2012
[13]. Arnoux, G. et al., HTPD 2012
[14]. T Eich, et al., Plasma Physics and Controlled Fusion, **49**, pp573-604, May 2007
[15]. Cenedese, A., et al., Fusion Eng. and Design, Vol.**66-68**, no.0, pp. 785 – 790, 2003. [Online];
[16]. D. Alves et al., Proceedings of the 13th ICALEPCS, Grenoble (2011);
[17]. van der Beken H. et al., Fusion Engineering, 1989. Proceedings., IEEE Thirteenth Symposium on, 2-6 1989, pp. 201 –204 vol.1.

	Expected power density (MW/m^2)	Expected ΔT (^oC)	Measured ΔT (^oC)
High elongation (Pulse No: 82359)	0.963	200	60
Low elongation (Pulse No: 81754)	0.686	142	20

Table 1:

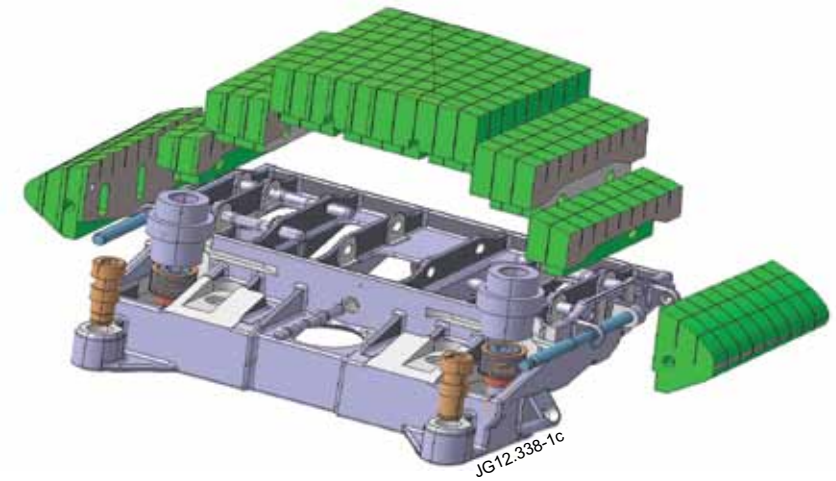

Figure 1: CATIA drawing of the outer poloidal limiter tile showing the segments and castellations.

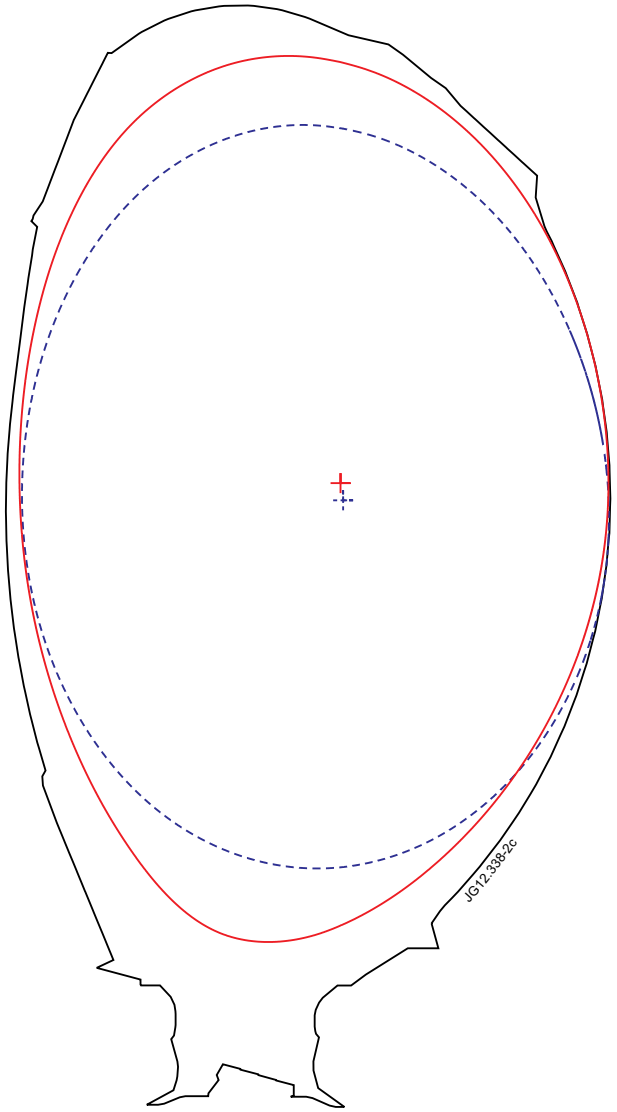

Figure 2: Limiter plasma configurations used for the power handling experiments.

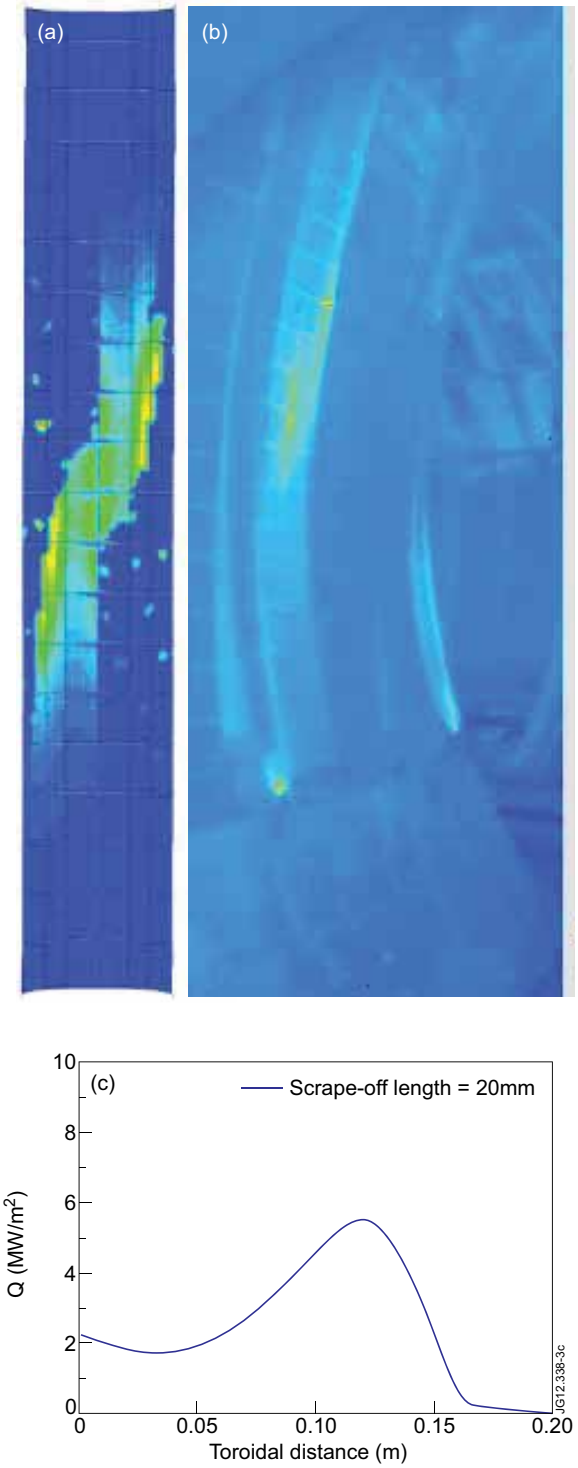

Figure 3: (a) Simulation of the heat flux distribution using a field line following code, (b) IR measurements of surface temperature and (c) analytical calculations for the IWGL.

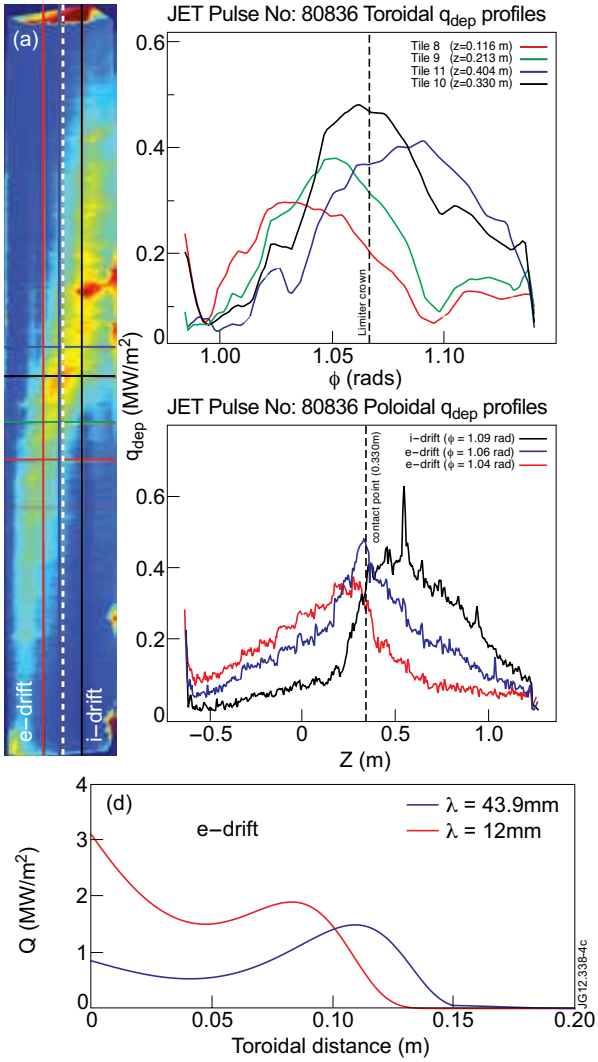

Figure 4: Power density assessment for an ohmic pulse using IR measurements to calculate (a) the power density at the limiter surface (b) toroidal profiles (c) poloidal profiles at a given position and (d) analytical calculations.

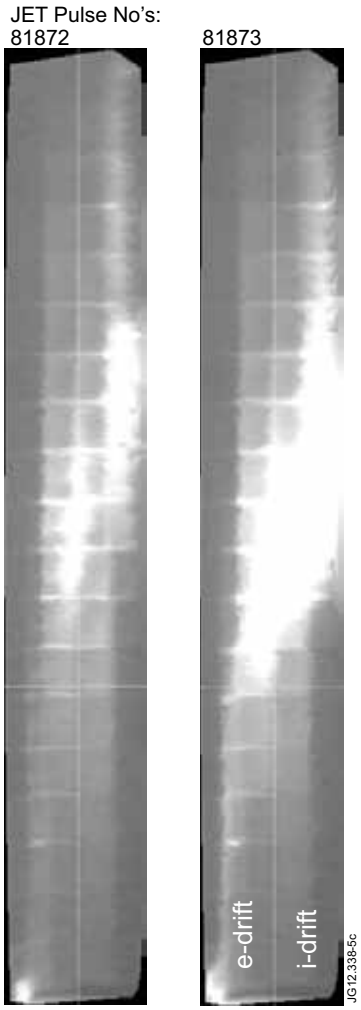

Figure 5:Effect of field line angle on shadowing.

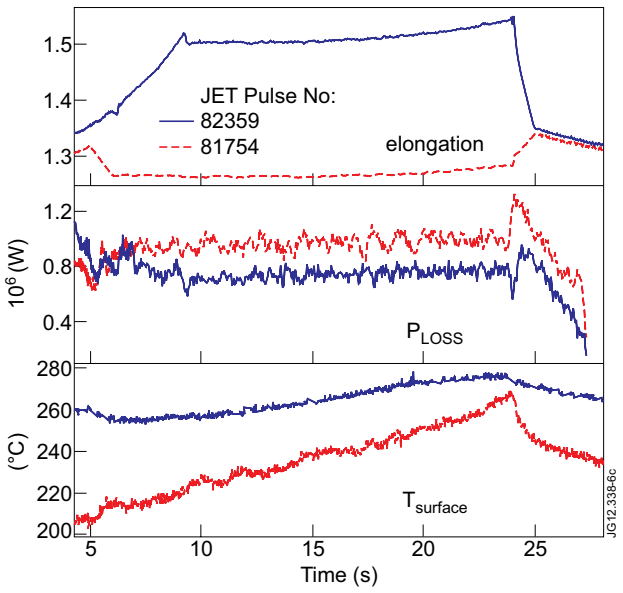

Figure 6: Surface temperature measurement for low and high elongated plasmas.

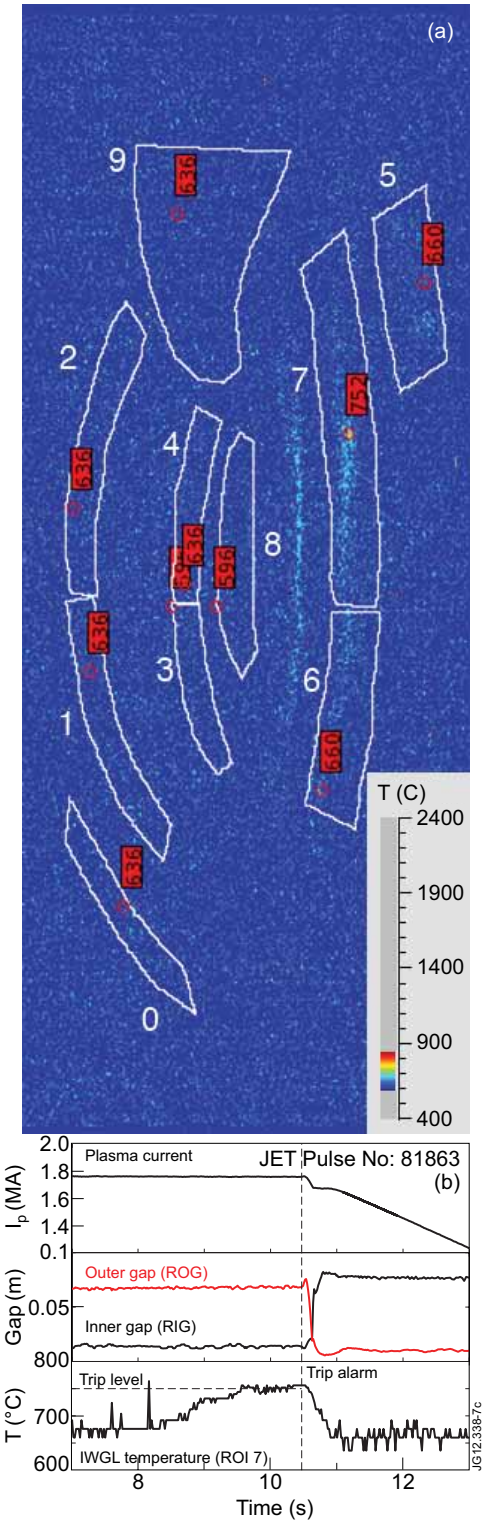

Figure 7:Definition of regions of interest and example of a stop issued by real time protection system due to a main chamber hot-spot (>750^{o}C, operational limit).

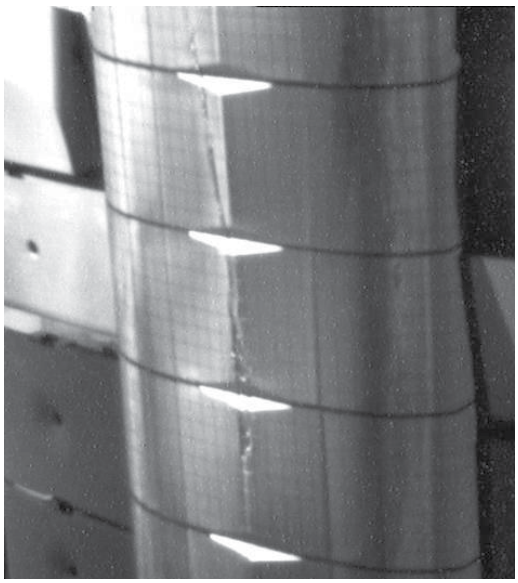

Figure 8:Thermal damage on the inner wall guard limiter.